Title

Fluorescently labeled chimeric anti-CEA antibody improves detection and resection of human colon cancer in a patient-derived orthotopic xenograft (PDOX) nude mouse model

Journal

Journal of Surgical Oncology, 109(5)

ISSN

8756-0437

Authors

Metildi, Cristina A
Kaushal, Sharmeela
Luiken, George A
et al.

Publication Date

2014-04-01

DOI

10.1002/jso.23507

Peer reviewed

Published in final edited form as:
J Surg Oncol. 2014 April ; 109(5): 451–458. doi:10.1002/jso.23507.

Fluorescently-labeled chimeric anti-CEA antibody improves detection and resection of human colon cancer in an orthotopic nude mouse model

Cristina A. Metildi, MD[1], **Sharmeela Kaushal, PhD**[1], **George A. Luiken, MD**[2], **Mark A. Talamini, MD**[1], **Robert M. Hoffman, PhD**[1,3], and **Michael Bouvet, MD**[1,4]

[1]University of California San Diego, Department of Surgery

[2]OncoFluor, Inc, San Diego

[3]AntiCancer, Inc., San Diego

[4]San Diego VA Medical Center, San Diego

Abstract

Background and Objectives—The aim of this study was to evaluate a new fluorescently labeled chimeric anti-CEA antibody for improved detection and resection of colon cancer.

Methods—Frozen tumor and normal human tissue samples were stained with chimeric and mouse antibody-fluorophore conjugates for comparison. Mice with patient-derived orthotopic xenografts (PDOX) of colon cancer underwent fluorescence-guided surgery (FGS) or bright-light surgery (BLS) 24 hours after tail vein injection of chimeric anti-CEA antibody. Resection completeness was assessed using postoperative images. Mice were followed for 6 months for recurrence.

Results—The fluorophore conjugation efficiency (dye:mole ratio) improved from 3–4 to >5.5 with the chimeric CEA antibody compared to mouse anti-CEA antibody. CEA-expressing tumors labeled with chimeric CEA antibody provided a brighter fluorescence signal on frozen human tumor tissues (p=0.046) and demonstrated consistently lower fluorescence signals in normal human tissues compared to mouse antibody. Chimeric CEA antibody accurately labeled PDOX colon cancer in nude mice, enabling improved detection of tumor margins for more effective FGS. The R0 resection rate increased from 86% to 96% with FGS compared to BLS.

Conclusion—Improved conjugating efficiency and labeling with chimeric fluorophore-conjugated antibody resulted in better detection and resection of human colon cancer in an orthotopic mouse model.

Keywords

colon cancer; orthotopic mouse models; chimeric antibody; fluorescence-guided surgery

Introduction

Surgical resection for colorectal cancer (CRC) has the greatest potential for cure. Since the application of complete mesocolic excision for colon cancer surgery, local 5-year recurrence rates have also decreased [1]. Furthermore, a proper oncologic approach in the surgical

Corresponding Author: Michael Bouvet, MD, Department of Surgery, Moores UCSD Cancer Center, 3855 Health Science Drive #0987, La Jolla, CA 92093-0987, Phone: 858-822-6191, Fax: 858-822-6192, mbouvet@ucsd.edu.

treatment of patients with CRC that involves not only achieving negative microscopic margins but also complete resection of metastatic tumor (R0 resection), can significantly improve 5-year survival rates [2–6].

Despite the high R0 resection rates in patients with colorectal cancer (CRC), local and distant recurrence is still a significant problem and has been cited as high as 34% [3,7,8]. One of the main causes of local recurrence is inadequate excision of the primary tumor or draining lymph nodes. Furthermore, the prognosis of patients with local recurrence is poor [9]. A real-time, reliable imaging technology for detection of positive surgical margins at the time of surgery would result in improved outcomes.

We have previously shown improved detection and resection of primary pancreatic cancer with a mouse-derived monoclonal fluorophore-conjugated antibody against carcino-embryonic antigen (CEA) in open laparotomies in mouse models [10]. In another study, we showed that fluorescence-guided surgery of green fluorescent protein (GFP)-expressing human colon cancer increased complete resection resulting in cures in an orthotopic nude mouse models [11,12]. The aim of the current study was to evaluate a fluorescent chimeric mouse-human antibody against CEA in a patient-derived orthotopic xenograft (PDOX) nude mouse model of colon cancer [13] for improved detection and resection, as a bridge to the clinic.

Materials & Methods

Antibody conjugation

Chimeric and mouse monoclonal antibodies specific for CEA were obtained from Aragen Bioscience, Inc. (Morgan Hill, CA). The antibody was labeled with the AlexaFluor 488 or 647 Protein Labeling Kit (Molecular Probes Inc., Eugene, OR) according to the manufacturer's instructions. Briefly, the monoclonal antibody was reconstituted at 2 mg/mL in PBS. 500 μL of the 2 mg/mL solution plus 50 μL of 1M sodium bicarbonate was added to the reactive dye and allowed to incubate for 1 hour at room temperature, then overnight at 4°C. The conjugated antibody was then separated from the remaining unconjugated dye on a purification column by centrifugation [14]. Antibody and dye concentrations in the final sample were determined using spectrophotometric absorbance with a Nanodrop ND 1000 spectrophotometer.

Tissue Sample Staining with Antibody Conjugates

Frozen human tumor and normal tissue arrays were purchased from Biochain Institute Inc. (Newark, CA). The tissue array was initially fixed in ice-cold acetone for 2 min, then air-dried and rehydrated with PBS. Slides were then incubated with 5% bovine serum albumin (BSA; Sigma-Aldrich, St Louis, MO) for 1 hour at room temperature. Using 1 μg/mL AlexaFluor 488 conjugated mouse or chimeric anti-CEA, or AlexaFlour 488 conjugated isotype control IgG. Slides were stained and allowed to incubate for 2 hours at room temperature. Prior to imaging, the slides were washed three times with PBS. An inverted DE-300 fluorescence microscope (Nikon, Tokyo, Japan) was used to obtain images of the antibody-stained slides.

Animal care

Female athymic nu/nu nude mice (AntiCancer, Inc, San Diego, CA) were bred and maintained in a barrier facility on high-efficiency particulate air filtered racks. The animals were fed with autoclaved laboratory rodent diet (Teckland LM-485; Western Research Products, Orange, CA). All surgical procedures were performed under anesthesia with an intramuscular injection of 100 μL of a mixture of 100 mg/kg ketamine and 10 mg/kg

xylazine. For each procedure, 20 μL of 1 mg/kg buprenorphine was administered for pain control. Euthanasia was achieved by 100% carbon dioxide inhalation, followed by cervical dislocation. All animal studies were conducted in accordance with the principles and procedures outlined in the National Institutes of Health (NIH) Guide for the Care and Use of Animals under assurance number A3873-01.

Subcutaneous Tumor Implantation

A human patient CEA-expressing colon cancer was excised under standard sterile conditions in the operating room by a surgical oncologist. After processing for histological evaluation in the pathology lab, the tumor was placed in PBS and properly transferred per standard protocols under an approved IRB with informed consent from the patient for generation of xenograft models. Tumor fragments were implanted subcutaneously within 30 min of harvesting over the right and left upper and lower flanks in female nu/nu mice between 4 and 6 weeks of age. Subcutaneous tumors were allowed to grow for 2–4 weeks until large enough to supply adequate tumor for orthotopic implantation.

Labeling of CEA-Expressing Human Patient Colon Tumor

A small portion of human patient CEA-expressing tumor not implanted into nude mice, was stored in OCT and later sectioned for fluorescence labeling with either the chimeric, mouse or control IgG antibody. Eight-micrometer thick sections of the frozen sample were fixed onto slides in preparation for staining. The slides were prepared and stained similar to the tissue arrays described earlier.

Orthotopic Tumor Implantation

Orthotopic human colon cancer xenografts were established in nude mice by direct surgical implantation of single 1 mm^3 tumor fragments from the subcutaneous xenografted tumors [13,15]. The cecum was delivered through a small 6 to 10-mm midline abdominal incision and the tumor fragment was sutured to the mesenteric border of the cecal wall using 8-0 nylon surgical sutures. Upon completion, the cecum was returned to the abdomen and the incision was closed in two layers using 6.0 Ethibond non-absorbable sutures (Ethicon Inc., Somerville, NJ).

Tumor Resection

A total of 43 mice were used in the experiments; 22 of them underwent fluorescence-guided surgery (FGS) and the other 21 mice underwent bright light surgery (BS). Timing of surgical resection was dependent on a specific tumor size criterion of 2–4 mm diameter after implantation. The human patient colon tumor displayed variable growth rates resulting in a variation in time points of tumor resection. Two to four weeks following orthotopic implantation, tumor-bearing mice were randomly assigned to the bright light surgery (BS) group or to the fluorescence-guided surgery (FGS) group. Use of a human patient colon cancer provided a heterogeneous orthotopic mouse population more representative of clinical CRC than the use of a cell line.

All mice received a tail vein injection of 75 μg of chimeric anti-CEA-Alexa 488 24 hours prior to planned resection of the colon tumor. This was to allow for accurate assessment of preoperative tumor burden for comparison among the surgical groups. Prior to resection of the colon tumor, mice were anesthetized as described, and their abdomens were sterilized. The cecum was delivered through a midline incision and the exposed colon tumor was imaged preoperatively with an OV-100 Small Animal Imaging System (Olympus Corp, Tokyo Japan), under both standard bright field and fluorescence illumination [16]. Resection of the primary colon tumor was performed using an MVX-10 fluorescence-dissecting

microscope (Olympus Corp) [17] under bright light illumination for the BS group and under fluorescence illumination, through a GFP filter (excitation HQ 470/10m, emission 525/50m), for the FGS group. The cecal stump was then sutured closed in a running fashion with 8-0 nylon surgical sutures [11]. Postoperatively, the surgical resection bed was imaged with the OV-100 under both standard bright-field and fluorescence illumination to assess completeness of surgical resection.

Post-surgical animal imaging

In order to assess for recurrence and to follow tumor progression postoperatively, the mice were injected with an anti-CEA antibody conjugated to Alexa 647. Mice were first imaged at two weeks and then at one month postoperatively, and monthly thereafter. Imaging took place 24 and 48 hrs after tail vein injection of the chimeric antibody conjugate. Whole body imaging of the mice was performed with the OV-100 containing an MT-20 light source (Olympus Biosystems, Planegg Germany) and DP70 CCD camera (Olympus Corp.) [16]. The mice were followed for 6 months postoperatively or until premorbid, whichever occurred first, at which point the mice were sacrificed 24 hours after intravenous injection of the chimeric anti-CEA-647 antibody. Intravital and ex vivo images were taken to evaluate the presence of local and/or distant recurrence. Premorbidity was determined by the degree of ascites, cachexia and/or mobility on a scale of 0 to 4 (4 being the highest grade). When ascites and cachexia and/or mobility reached a grade of 4, the mouse was sacrificed. All images were analyzed with Image J v1.440 (National Institutes of Health, Bethesda, MD).

Tissue histology

For correlation of surgical findings with histology, tumor samples were removed with surrounding normal tissues at the time of resection. Fresh tissue samples were fixed in Bouin solution and regions of interest embedded in paraffin prior to sectioning and staining with H&E for standard light microscopy. H&E-stained permanent sections were examined using a BX41 microscope (Olympus Corp) equipped with a Micropublisher 3.3 RTV camera (QImaging, Surrey, B.C., Canada). All images were acquired using QCapture software (QImaging) without post-acquisition processing.

Data processing & statistical analysis

PASWStatistics 18.0 (SPSS, Inc.) was used for all statistical analyses. Tumor burden was expressed as mean ± SEM. A Student's t-test was used to compare continuous, normally-distributed variables between two groups; a nonparameteric Wilcoxon rank sum test was used to compare treatment groups with data that were not normally distributed. Comparisons between categorical variables were analyzed using Fisher's exact tests. A p-value of ≤ 0.05 was considered statistically significant for all comparisons.

Results

Conjugation Efficiency

The conjugation efficiency of the chimeric anti-CEA antibody was compared to the mouse antibody. Conjugation consistently resulted in a dye to mole ratio of 3–4 when using the monoclonal mouse antibody. Conjugating the chimeric form of the anti-CEA antibody to Alexa 488 resulted in ratios >5.5 and >10 when conjugating to Alexa 647. Thus the chimeric antibody resulted in improved conjugating efficiency.

Labeling Efficacy of Frozen Human Tissue Arrays with Chimeric vs Mouse Antibody

Prior to testing the chimeric antibody in our mouse models of CEA-expressing human colon cancer, preliminary in vitro staining studies were carried out. Frozen human tumor and

normal tissue arrays were stained with either the mouse or chimeric anti-CEA-Alexa 488 antibody (Figure 2a and 2b, respectively). Images were taken and the level of fluorescence signal intensity was measured. Both antibodies demonstrated specific labeling to CEA-expressing colon, lung and pancreas tumor tissue. Furthermore, normal liver and lung tissue, and even less so, pancreas tissue, demonstrated minimal fluorescence labeling with both antibody forms.

For more objective comparison, fluorescence signal intensity was calculated from the fluorescence microscopy images taken of each positively stained sample. Tumor tissue from colon, pancreas and lung stained with the chimeric antibody conjugate had significantly greater overall mean fluorescence signal intensities compared to the respective samples stained with the mouse antibody conjugate (95.2 ± 6.02 vs 71.0 ± 5.93; $p=0.046$), indicating improved binding and thus greater sensitivity of the chimeric antibody in labeling CEA-expressing tumors compared to the mouse antibody (Figure 3a).

An antibody conjugate's ability to specifically identify tumor tissue from normal surrounding tissue in which the tumor resides is the most important indication of the accuracy of the antibody. Normal pancreas, colon and lung tissue of the frozen human tissue array demonstrated low levels of fluorescence staining with both forms on the anti-CEA antibody. The mean fluorescence signal intensity of normal tissue samples was calculated for comparison. The chimeric form yielded consistently lower signals compared with the mouse antibody (normal colon tissue: 4.3 vs 5.4, respectively; normal pancreas tissue: 1.5 vs 2.7, respectively; normal lung tissue: 12.1 vs 13.7, respectively) (Figure 3a). Despite having a greater dye:mole ratio and thus better conjugating efficiency, the specificity of the chimeric antibody resulted in a lower fluorescence signal in normal human tissue.

Labeling Efficacy of Human CEA-Expressing Colon Tumor

The next objective was to evaluate labeling efficacy of the chimeric antibody in a patient-derived orthotopic xenograft (PDOX) mouse model of CEA-expressing colon cancer. Prior to any in vivo labeling, we compared binding of the two different antibodies to the PDOX frozen sections (Figure 3b). We also compared the anti-CEA-Alexa 488 antibodies to a negative control, IgG-Alexa 488, antibody. The fluorescence signal intensity generated by labeling the tumor tissue increased from 59.7 with the mouse antibody to 80.4 with the chimeric antibody ($p<0.001$). As expected, there was very minimal labeling with the negative control IgG antibody.

Subcutaneous models of the CEA-expressing human patient colon tumor were generated in nude mice by implanting fragments of the freshly excised tumor just below the skin into upper and lower bilateral flanks. Tumor was allowed to grow for 4 weeks prior to any testing. Twenty-four hours prior to imaging, mice harboring subcutaneous tumors were injected via tail vein with 75 μg of either the anti-CEA-Alexa 488 chimeric antibody or mouse antibody. Initially, whole body imaging was performed and then skin flaps were generated and images with the OV-100 were obtained (Figure 4). Fluorescence signal intensities of fluorescently-labeled tumors were calculated from the skin flap images. The average fluorescence signal intensity increased from 95 yielded by labeling with the mouse antibody to 106 with the chimeric antibody ($p=0.083$). Lack of statistical significance was most likely due to lack of statistical power with a low sample number.

Fluorescence-Guided Surgery with Chimeric Antibody

The final objective was to evaluate the efficiency of the chimeric antibody conjugate for FGS in the PDOX model. The chimeric antibody conjugated to Alexa 488 demonstrated accurate and specific labeling of the orthotopic tumor in the PDOX model. The sensitivity

and specificity of the antibody permitted visualization of sub-millimeter, microscopic tumor deposits along the wall of the cecum (Figure 5) that were not visualized in the bright field images. A complete resection was evident by the absence of any fluorescence signal in postoperative images. The improved visualization and real-time detection of tumor with fluorescence labeling of the chimeric antibody permitted an increase in complete resection rates compared to standard bright light surgery from 85.7% to 95.5% (Figure 6).

Discussion

Surgical resection of all cancerous tissue when possible and achieving an R0 resection is the single most important factor that offers the best opportunity for cure and thus long-term survival in patients. While true for most solid cancers, this is particularly important in colorectal cancer. Campos, et al. [3] described the significant impact on survival of achieving an R0 resection through a radical resection in patients with locally advanced colorectal cancer. In addition, the standardization of complete mesocolic excision as a surgical technique for patients with colon cancer in some institutions has subsequently reduced local 5-year recurrence rates and improved survival [1,18,19]. Furthermore, resection of liver and pulmonary metastases in selected cases with intent for cure has significantly enhanced 5-year survival rates [4,6,20,21]. Being one of the most frequent malignant tumors in the Western world, with a incidence of local invasion or adhesion to surrounding organs in 5–20% of cases [3], or metastasis to the liver in up to 25% of patients at time of diagnosis [22], and in which recurrence is still a significant issue after curative intent, improved operative strategies are needed to enhance to a surgeon’s ability to achieve an R0 resection.

In addition, peritoneal carcinomatosis from colorectal cancer is associated with a significantly poor survival ranging from 5 to 7 months. Historically, there have been few therapeutic or palliative options available to these patients [23–25]. Cytoreductive surgery (CRS) combined with hyperthermic intraperitoneal chemotherapy (HIPEC) has been shown in clinical trials to significantly improve median survival compared to systemic chemotherapy alone or with palliative surgery [26,27]. The recently published Dutch trial [28], in which 960 enrolled patients underwent CRS and HIPEC, demonstrated tolerable morbidity with improved survival. The survival advantage of CRS with HIPEC over systemic chemotherapy with palliative surgery can be attributed to significant debulking of tumor. The improved survival advantage experienced by the enrolled patients parallels the complete resection rates achieved in these trials. Fluorescence-guided surgery provides the operating surgeon with real-time, objective means of identifying not only tumor margins but also metastatic lesions and peritoneal deposits which enhance the surgeon’s ability to completely resect all visible tumor.

Another potential impact of fluorescence-guided surgery lies in laparoscopic approach to resect colorectal cancer. The surgeon must rely on preoperative imaging, colonoscope findings and ink markings to locate the tumor intraoperatively. While colonoscopy is a highly sensitive modality used for colorectal cancer screening, it has been reported in the literature to have a miss rate as high as 24% [29–31]. In these studies evaluating the efficacy of colonoscopy as a screening tool, it was the smaller (<1 cm) and right-sided adenomas that were more likely to be missed, calling for further improvement of colonoscopic techniques and technologies. Fluorescently labeling tumor can enhance detection and localization of tumor on colonoscopy and during laparoscopic surgery where visual cues without tactile sense are the only tools available to the gastroenterologist or surgeon.

In a previous study, we demonstrated improved surgical outcomes with fluorescence-guided surgery in mouse models of human colon cancer in which a higher rate of complete

resection was achieved that translated into longer overall survival [11]. Recurrence rates were significantly decreased by FGS and mice in the FGS group experienced longer disease-free survival. We also demonstrated significantly greater tumor reduction and debulking in mouse models of peritoneal carcinomatosis of human colon cancer. However, the human colon cancer lines used in this study were genetically engineered in vitro to express GFP before implantation in mouse models. In a more recent study, we used fluorophore-conjugated monoclonal mouse antibodies against CEA to fluorescently label CEA-expressing pancreatic cancer for surgical resection in mouse models [32]. Again, we demonstrated improved surgical outcomes with a more clinically-applicable method of fluorescence-guided surgery, with the use of fluorophore-conjugated antibodies.

The aim of the present study was to develop a more clinically relevant antibody that maintained its sensitivity and specificity to the target for future use in human patient trials of FGS. As non-human proteins, monoclonal mouse antibodies tend to evoke an immune reaction when administered to humans. Creating a “fusion” protein allows introduction of segments of human constant domains while maintaining important properties from the “parent” mouse protein, eliminating most of the potentially immunogenic portions of the antibody without compromising its specificity for the intended target [33]. There are currently several chimeric protein FDA-approved drugs available for clinical use, such as Rituximab (Rituxan), Basiliximab (Simulect), and Infliximab (Remicade) with many more currently being developed for cancer therapy [34–36].

The ability to visualize primary tumor as well as small satellite tumors near the surgical margin that virtually go undetected under standard bright light surgery has had a significant impact in surgical outcomes in mouse models [10,11,14,37–43]. We demonstrated in the current study that failure to remove these small deposits in the BLS group resulted in recurrence in a matter of months. Providing a more objective method of detecting tumor intraoperatively for better delineation of tumor from normal surrounding tissue can permit a more precise excision. Future experiments will determine whether the fluorescently labeling the tumor will also reduce the operative time.

The patient colon tumor used was not genetically fluorescent and therefore postoperative follow-up to assess for local and distant recurrence proved difficult. To address this, monthly injections of the anti-CEA-Alexa 647 antibody were given intravenously and whole body imaging was performed at 24 and 48 hour time points. Repeated injections however resulted in saturation of the tumor antigen and with natural dissociation of the conjugate dye from the antibody and therefore fluorescence labeling became less accurate for tumor detection upon whole body imaging. However, this study demonstrated improved labeling of CEA-expressing tumor tissue with the chimeric form of an anti-CEA-Alexa 488 antibody to the mouse form previously used in animal studies. The current study further demonstrated the utility of chimeric antibodies for future large animal studies and subsequent human trials to evaluate the clinical efficacy of fluorescence-guided surgery. Although the standard segmental colon-cancer resection in early disease may not need fluorescence labeling of the tumor, resection of locally-advanced disease as well as local, regional and metastatic recurrent disease should be greatly improved with the labeling techniques described in the present study.

Conclusion

A chimeric fluorophore-conjugated CEA antibody demonstrated more effective labeling of human CEA-expressing cancer in tissue arrays and in PDOX nude models of human patient colon cancer. Fluorescently labeling tumor with the chimeric antibody permitted real-time detection of tumor margins that resulted in better complete resection rates in PDOX models.

The improved effectiveness of the chimeric fluorophore-conjugated anti-CEA antibody should enable fluorescence-guided surgery of cancer in the clinic.

Acknowledgments

Work supported in part by grants from the National Cancer Institute CA142669 and CA132971 (to M.B. and AntiCancer, Inc) and T32 training grant CA121938-5 (to C.A.M.).

References

1. Hohenberger W, Weber K, Matzel K, et al. Standardized surgery for colonic cancer: complete mesocolic excision and central ligation--technical notes and outcome. Colorectal Dis. 2009; 11:354–364. discussion 364–355. [PubMed: 19016817]
2. Andreoni B, Chiappa A, Bertani E, et al. Surgical outcomes for colon and rectal cancer over a decade: results from a consecutive monocentric experience in 902 unselected patients. World J Surg Oncol. 2007; 5:73. [PubMed: 17610720]
3. Campos FG, Calijuri-Hamra MC, Imperiale AR, et al. Locally advanced colorectal cancer: results of surgical treatment and prognostic factors. Arq Gastroenterol. 2011; 48:270–275. [PubMed: 22147133]
4. Mayo SC, Pulitano C, Marques H, et al. Surgical management of patients with synchronous colorectal liver metastasis: a multicenter international analysis. J Am Coll Surg. 2013; 216:707–716. discussion 716–708. [PubMed: 23433970]
5. Ruo L, Guillem JG. Surgical management of primary colorectal cancer. Surg Oncol. 1998; 7:153–163. [PubMed: 10677166]
6. Yedibela S, Klein P, Feuchter K, et al. Surgical management of pulmonary metastases from colorectal cancer in 153 patients. Ann Surg Oncol. 2006; 13:1538–1544. [PubMed: 17009154]
7. Manfredi S, Benhamiche AM, Meny B, et al. Population-based study of factors influencing occurrence and prognosis of local recurrence after surgery for rectal cancer. Br J Surg. 2001; 88:1221–1227. [PubMed: 11531871]
8. Manfredi S, Bouvier AM, Lepage C, et al. Incidence and patterns of recurrence after resection for cure of colonic cancer in a well defined population. Br J Surg. 2006; 93:1115–1122. [PubMed: 16804870]
9. Abulafi AM, Williams NS. Local recurrence of colorectal cancer: the problem, mechanisms, management and adjuvant therapy. Br J Surg. 1994; 81:7–19. [PubMed: 8313126]
10. Tran Cao HS, Kaushal S, Metildi CA, et al. Tumor-specific fluorescence antibody imaging enables accurate staging laparoscopy in an orthotopic model of pancreatic cancer. Hepatogastroenterology. 2012; 59:1994–1999. [PubMed: 22369743]
11. Metildi CA, Kaushal S, Snyder CS, et al. Fluorescence-guided surgery of human colon cancer increases complete resection resulting in cures in an orthotopic nude mouse model. J Surg Res. 2013; 179:87–93. [PubMed: 23079571]
12. Kishimoto H, Zhao M, Hayashi K, et al. In vivo internal tumor illumination by telomerase-dependent adenoviral GFP for precise surgical navigation. Proc Natl Acad Sci U S A. 2009; 106:14514–14517. [PubMed: 19706537]
13. Fu XY, Besterman JM, Monosov A, Hoffman RM. Models of human metastatic colon cancer in nude mice orthotopically constructed by using histologically intact patient specimens. Proc Natl Acad Sci U S A. 1991; 88:9345–9349. [PubMed: 1924398]
14. Kaushal S, McElroy MK, Luiken GA, et al. Fluorophore-conjugated anti-CEA antibody for the intraoperative imaging of pancreatic and colorectal cancer. J Gastrointest Surg. 2008; 12:1938–1950. [PubMed: 18665430]
15. Hoffman RM. Orthotopic metastatic mouse models for anticancer drug discovery and evaluation: a bridge to the clinic. Invest New Drugs. 1999; 17:343–359. [PubMed: 10759402]
16. Yamauchi K, Yang M, Jiang P, et al. Development of real-time subcellular dynamic multicolor imaging of cancer-cell trafficking in live mice with a variable-magnification whole-mouse imaging system. Cancer Res. 2006; 66:4208–4214. [PubMed: 16618743]

17. Kimura H, Momiyama M, Tomita K, et al. Long-working-distance fluorescence microscope with high-numerical-aperture objectives for variable-magnification imaging in live mice from macro- to subcellular. J Biomed Opt. 2010; 15:066029. [PubMed: 21198203]
18. Bokey EL, Chapuis PH, Dent OF, et al. Surgical technique and survival in patients having a curative resection for colon cancer. Dis Colon Rectum. 2003; 46:860–866. [PubMed: 12847357]
19. Jagoditsch M, Lisborg PH, Jatzko GR, et al. Long-term prognosis for colon cancer related to consistent radical surgery: multivariate analysis of clinical, surgical, and pathologic variables. World J Surg. 2000; 24:1264–1270. [PubMed: 11071473]
20. Misiakos EP, Karidis NP, Kouraklis G. Current treatment for colorectal liver metastases. World J Gastroenterol. 2011; 17:4067–4075. [PubMed: 22039320]
21. Sharma S, Camci C, Jabbour N. Management of hepatic metastasis from colorectal cancers: an update. J Hepatobiliary Pancreat Surg. 2008; 15:570–580. [PubMed: 18987925]
22. Small R, Lubezky N, Ben-Haim M. Current controversies in the surgical management of colorectal cancer metastases to the liver. Isr Med Assoc J. 2007; 9:742–747. [PubMed: 17987765]
23. Jayne DG, Fook S, Loi C, Seow-Choen F. Peritoneal carcinomatosis from colorectal cancer. Br J Surg. 2002; 89:1545–1550. [PubMed: 12445064]
24. Koppe MJ, Boerman OC, Oyen WJ, Bleichrodt RP. Peritoneal carcinomatosis of colorectal origin: incidence and current treatment strategies. Ann Surg. 2006; 243:212–222. [PubMed: 16432354]
25. Sadeghi B, Arvieux C, Glehen O, et al. Peritoneal carcinomatosis from non-gynecologic malignancies: results of the EVOCAPE 1 multicentric prospective study. Cancer. 2000; 88:358–363. [PubMed: 10640968]
26. Franko J, Ibrahim Z, Gusani NJ, et al. Cytoreductive surgery and hyperthermic intraperitoneal chemoperfusion versus systemic chemotherapy alone for colorectal peritoneal carcinomatosis. Cancer. 2010; 116:3756–3762. [PubMed: 20564081]
27. Verwaal VJ, van Ruth S, de Bree E, et al. Randomized trial of cytoreduction and hyperthermic intraperitoneal chemotherapy versus systemic chemotherapy and palliative surgery in patients with peritoneal carcinomatosis of colorectal cancer. J Clin Oncol. 2003; 21:3737–3743. [PubMed: 14551293]
28. Kuijpers AM, Mirck B, Aalbers AG, et al. Cytoreduction and HIPEC in The Netherlands: Nationwide Long-term Outcome Following the Dutch Protocol. Ann Surg Oncol. 2013
29. Bressler B, Paszat LF, Vinden C, et al. Colonoscopic miss rates for right-sided colon cancer: a population-based analysis. Gastroenterology. 2004; 127:452–456. [PubMed: 15300577]
30. Postic G, Lewin D, Bickerstaff C, Wallace MB. Colonoscopic miss rates determined by direct comparison of colonoscopy with colon resection specimens. Am J Gastroenterol. 2002; 97:3182–3185. [PubMed: 12492208]
31. Rex DK, Cutler CS, Lemmel GT, et al. Colonoscopic miss rates of adenomas determined by back-to-back colonoscopies. Gastroenterology. 1997; 112:24–28. [PubMed: 8978338]
32. Metildi CA, Kaushal S, Talamini MA, et al. Fluorophore-conjugated antibodies improve surgical resection of pancreatic cancer leading to prolonged disease-free survival and overall survival in orthotopic mouse models. J Am Coll Surg. 2012; 215:S127–S128.
33. Nelson AL, Dhimolea E, Reichert JM. Development trends for human monoclonal antibody therapeutics. Nat Rev Drug Discov. 2010; 9:767–774. [PubMed: 20811384]
34. Ho M, Royston I, Beck A. 2nd PEGS Annual Symposium on Antibodies for Cancer Therapy: April 30–May 1, 2012, Boston, USA. MAbs. 2012; 4:562–570. [PubMed: 22864478]
35. Beck A, Wurch T, Bailly C, Corvaia N. Strategies and challenges for the next generation of therapeutic antibodies. Nat Rev Immunol. 2010; 10:345–352. [PubMed: 20414207]
36. Reichert JM, Dhimolea E. The future of antibodies as cancer drugs. Drug Discov Today. 2012; 17:954–963. [PubMed: 22561895]
37. McElroy M, Kaushal S, Luiken GA, et al. Imaging of primary and metastatic pancreatic cancer using a fluorophore-conjugated anti-CA19–9 antibody for surgical navigation. World J Surg. 2008; 32:1057–1066. [PubMed: 18264829]
38. Metildi CA, Hoffman RM, Bouvet M. Fluorescence-guided surgery and fluorescence laparoscopy for gastrointestinal cancers in clinically-relevant mouse models. Gastroenterol Res Pract. 2013; 2013:290634. [PubMed: 23533387]

39. Metildi CA, Kaushal S, Hardamon CR, et al. Fluorescence-guided surgery allows for more complete resection of pancreatic cancer, resulting in longer disease-free survival compared with standard surgery in orthotopic mouse models. J Am Coll Surg. 2012; 215:126–135. discussion 135–126. [PubMed: 22632917]

40. Metildi CA, Kaushal S, Lee C, et al. An LED light source and novel fluorophore combinations improve fluorescence laparoscopic detection of metastatic pancreatic cancer in orthotopic mouse models. J Am Coll Surg. 2012; 214:997–1007. e1002. [PubMed: 22542065]

41. Tran Cao HS, Kaushal S, Lee C, et al. Fluorescence laparoscopy imaging of pancreatic tumor progression in an orthotopic mouse model. Surg Endosc. 2011; 25:48–54. [PubMed: 20533064]

42. Tran Cao HS, Kaushal S, Menen RS, et al. Submillimeter-resolution fluorescence laparoscopy of pancreatic cancer in a carcinomatosis mouse model visualizes metastases not seen with standard laparoscopy. J Laparoendosc Adv Surg Tech A. 2011; 21:485–489. [PubMed: 21699431]

43. Bouvet M, Hoffman RM. Glowing tumors make for better detection and resection. Sci Transl Med. 2011; 3:110fs110.

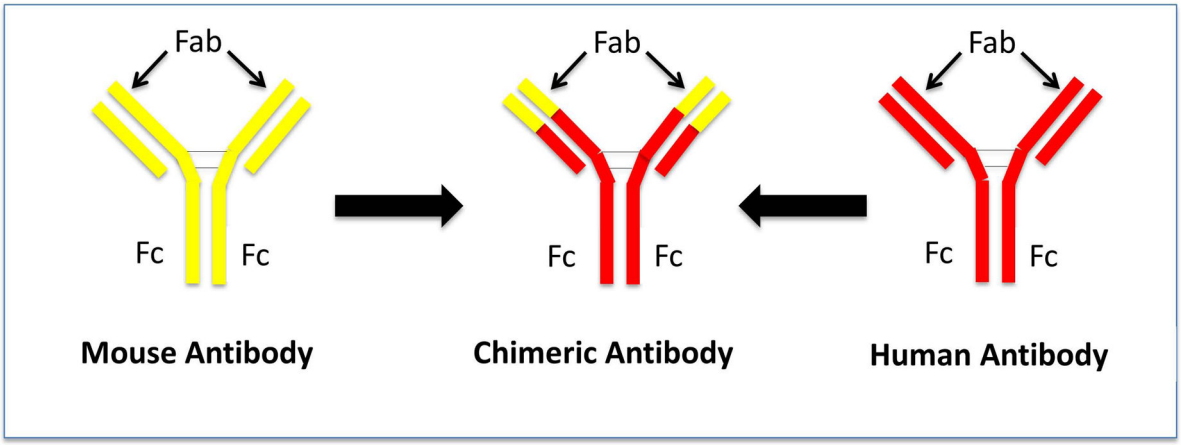

Figure 1. Process of chimerization of anti-CEA antibody

This diagram represents the process of making a mouse-human chimeric anti-CEA antibody (Aragen Biosciences, Inc.).

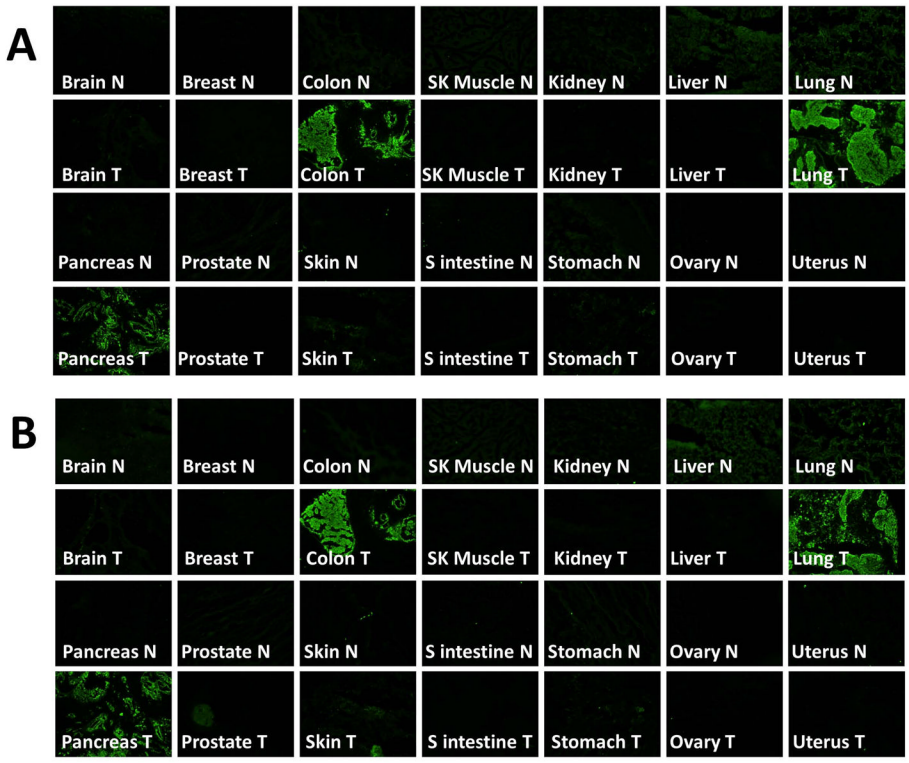

Figure 2. Frozen tumor and normal tissue array stained with mouse or chimeric anti-CEA- 488

A) This frozen tumor and normal human tissue array were labeled with the mouse anti-CEA-Alexa 488 antibody. Although there is some background labeling of normal liver and lung tissue, the fluorescence signal intensity is much greater in the labeled colon, lung and pancreas tumor tissues. N, normal; T, tumor **B)** In frozen tumor and normal human tissue array stained with the chimeric anti-CEA-Alexa 488 antibody, there was minimal labeling in the normal liver and lung tissue but significantly greater fluorescence signal intensity in labeled colon, lung and pancreas tumor tissues. N, normal; T, tumor

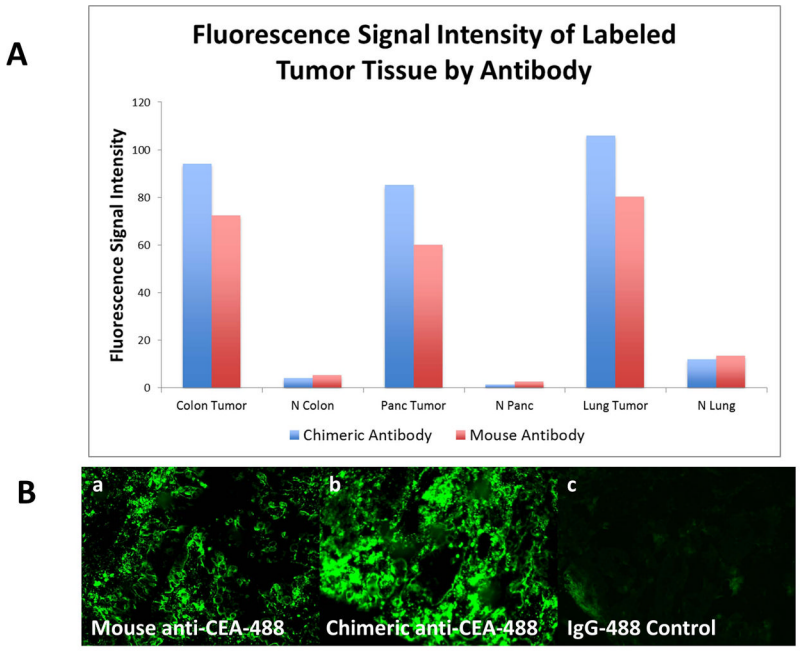

Figure 3. Fluorescence signal intensity of labeled frozen tumor and normal tissue by the mouse and chimeric anti-CEA antibodies

A) Staining of CEA-expressing frozen tumor tissue samples with the chimeric antibody conjugate gave a brighter fluorescence signal compared to staining with the mouse antibody conjugate ($p=0.046$). Despite the higher dye:mole ratio obtained with the chimeric antibody conjugate, a lower fluorescence signal intensity was consistently observed in the chimeric antibody-stained normal human tissue samples compared to mouse antibody-stained tissue. However, given the significantly brighter signal of chimeric antibody-labeled tumor, the contrast between normal tissue and tumor tissue achieved with the chimeric antibody was greater. N, normal. **B)** The human colon cancer tumor used to generate the PDOX nude-mouse models was stained with either mouse or chimeric anti-CEA-Alexa 488 antibody and compared to a negative control IgG-488 antibody. The chimeric antibody (b) demonstrated improved binding to the CEA-expressing colon cancer and thus yielded a significantly brighter fluorescence signal ($p<0.001$) compared to the sample labeled with the mouse antibody conjugate (a). As expected, there was no binding with the IgG-488 antibody.

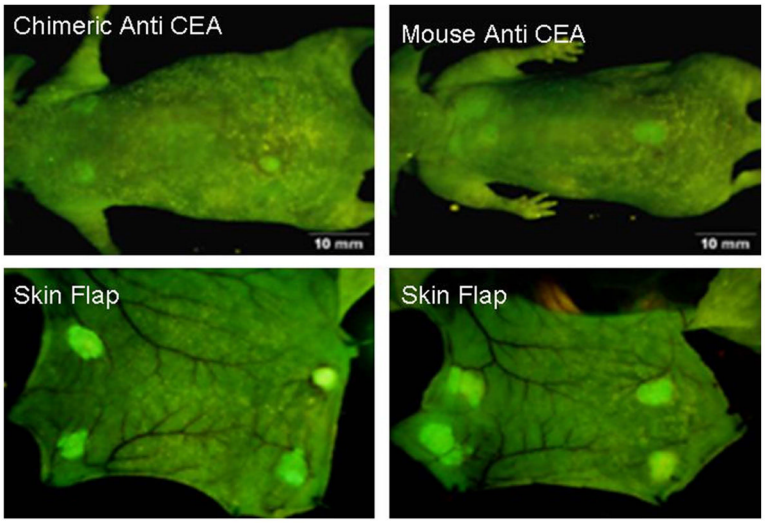

Figure 4. In situ labeling of subcutaneous implanted CEA-expressing human colon tumors with the anti-CEA chimeric antibody

Labeling with the chimeric anti-CEA antibody yielded a brighter fluorescence signal in the subcutaneous mouse models of the CEA-expressing patient colon cancer, increasing the fluorescence signal intensity from 95 with the mouse antibodies to 106 with the chimeric antibodies.

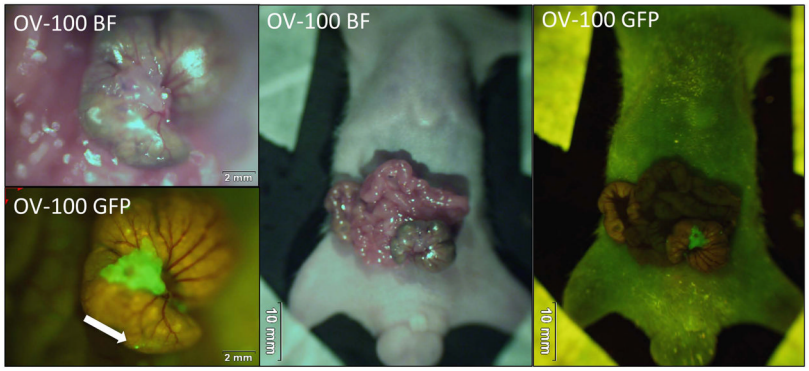

Figure 5. In situ labeling of CEA-expressing human colon cancer in orthotopic mouse models with the chimeric anti-CEA antibody

The chimeric antibody bound to the colon tumor thereby fluorescently labeling the tumor. As indicated by the white arrow, small microscopic, sub-millimeter tumor deposits were easily visualized by labeling with the chimeric antibody.

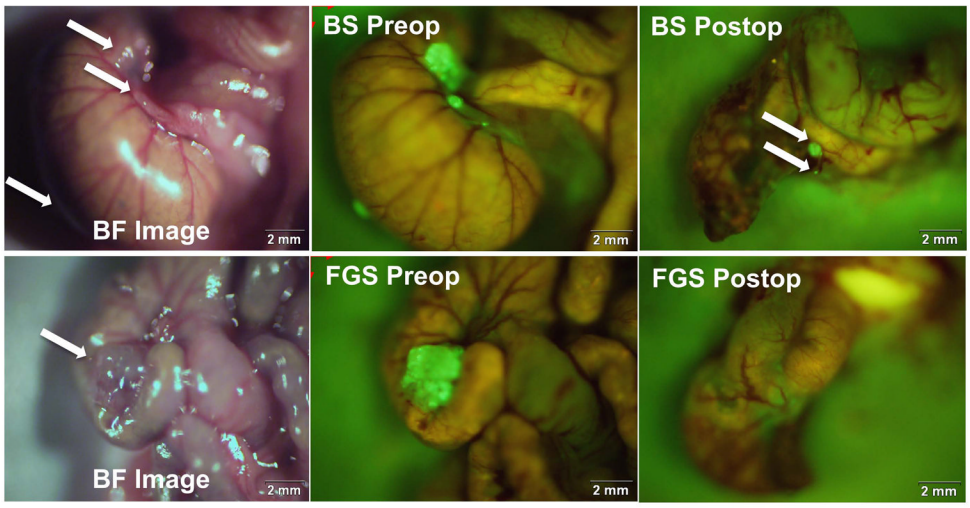

	BS	FGS
Complete Resection Rate	85.7% (18/21)	95.5% (21/22)

Figure 6. Pre- and postoperative images under fluorescence guided and bright-light surgery

Fluorescence-guided surgery (FGS) with the chimeric antibody improved real-time detection of tumor margins thereby increasing complete resections in the FGS group compared to the bright light surgery (BLS) group from 85.7% to 95.5%, respectively. Small tumor deposits (indicated by white arrows) remained in a mouse from the BLS group. The absence of any fluorescence signal in the mouse in the FGS group indicates a complete resection. The corresponding preoperative bright field images are on the left to better illustrate the difficulty of identifying tumor margins without fluorescence labeling. White arrows indicate tumor lesions in the wall of the cecum.